

A TOP-DOWN OPERATOR FOR THE AUTOMATIC EXTRACTION OF TREES - CONCEPT AND PERFORMANCE EVALUATION

Bernd-M. Straub

IPI, Institute of Photogrammetry and GeoInformation, University of Hannover
Nienburger Straße 1, 30167 Hannover, Germany, bernd-m.straub@ipi.uni-hannover.de

Commission III, WG 3

KEY WORDS: Forestry, Urban, Extraction, Algorithms, Scale Space, Automatic, Tree

ABSTRACT:

An approach for the automatic extraction of trees is presented. It is based on a multi-scale representation of a surface model in Linear Scale Space. The segmentation of the surface model is performed using a watershed transformation in multiple scale levels in order to detect trees of different size classes. The detection of the trees in the investigated scene is based on four parameters; three of them can be looked upon as object specific. Only one parameter depends on the raster data. The approach was applied to different data sets, surface models from laser scanner and from image matching, also. Urban and forest scenes were investigated.

1. INTRODUCTION

In this paper we present an approach for the automatic extraction of individual trees. A digital surface model is used as main source of information for the extraction of individual trees. Colour information from optical images is used, in order to differentiate between vegetation and other objects in the investigated scene.

The approach can be looked upon as a top-down low-level operator: Individual trees are extracted without a high level steering component, the number of steering parameters is comparatively small, and no assumptions regarding the context are made. Of course, this statement is only true in the application domain of the extraction of topographic objects from aerial/satellite images and surface models, not for terrestrial recordings. The trees must be visible from above in the image and 2.5D height data. Originally, the method was developed for the automatic extraction of trees in settlement areas from very high-resolution data: a surface model with a ground sampling distance (GSD) of 0.2 m and true orthoimages with 0.1 m GSD. An example of such a data set is depicted in Figure 1, it was acquired over Grangemouth, Scotland in summer 2000, refer (Straub & Heipke 2001) for details about the data set.

In order to investigate the potential of the approach, we applied it on three other data sets. The first one is called the *Hohentauern* data set, a test site in a forest in the Austrian Alps. The main species in this test site is spruce (94%). The laser scanner flight with a TopoSys I Scanner was carried out in August 1999 in Austria, close to Hohentauern. The flying altitude was approximately 800 m above ground, leading to 4-5 points per m². The Joanneum Research in Graz, Austria provided the data for this investigation. The second data set was captured in the April of 2001 with the TopoSys II sensor from about 830 m above ground in the south of Germany close to the city Ravensburg. This *Ravensburg* data set consists of a surface model with 1 m resolution and optical data with 0.5 m resolution. The TopoSys GmbH, Germany, made the

Ravensburg data set available¹. The third data set was acquired with the HRSC acquisition system by ISTAR in summer 1999 over *Paris*. The GSD of the three-line scanner was 0.5 m and the computed surface model has a GSD of 1 m. The data set was provided by ISTAR, France.

The paper is structured as follows: After a short overview on related work in the next section, a brief description of the approach is given. The next section is about the performance evaluation, including visual examples of two data sets. The paper closes with a short summary and an outlook on future work.

2. RELATED WORK

Trees are important topographic objects in different fields of applications. Not only ecological aspects constitute the interest in trees but also different economic factors. Obviously, data about trees are important in forest inventories and forestry GIS applications. In forest inventories trees are counted and parameters like height and stem diameter are measured. Recent work in the field was published in (Pollock 1996), (Brandtberg & Walter 1998), (Larsen 1999), (Andersen et al. 2002), (Persson et al. 2002), and (Schardt et al. 2002). An excellent state-of-the-art overview is given (Hill & Leckie 1999).

A common element of many approaches is the geometric model of a tree proposed by Pollock in (Pollock 1994). In the following, this surface description is assigned as *Pollock-Model*. Two different surfaces, which can be described with the Pollock-Model, are depicted in Figure 1: The left one is an example for a deciduous tree, and the right one for a coniferous.

¹ An overview about companies and sensors dealing with laser scanning gives (Baltsavias 1999).

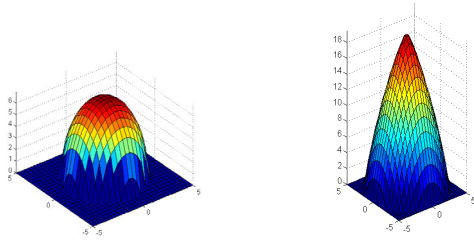


Figure 1: 3D visualisation of the Pollock-Model. Left: Surface model of a typical deciduous tree: $a=7$, $b=3.5$, $n=1.2$. Right: Coniferous tree: $a=20.0$; $b=5.0$; $n=1.2$.

In the real world, the surface of a tree is of course very noisy in comparison to the Pollock-Model. This noise is not caused by the measurement of the surface. It is simply a consequence of using such a model for a complex shape like the real crown of a tree. But the main shape of the crown is well modelled with this surface description.

Another common element in the most approaches is the application of the Linear Scale-Space in the early processing stages of the image analysis, for example (Dralle & Rudemo 1996), (Brandtberg & Walter 1998), (Schardt et al. 2002), and (Persson et al. 2002). In (Andersen et al. 2001) a morphological Scale-Space is used for the extraction of tree positions.

A basic idea of a Scale-Space in image analysis is to construct a multi-scale representation of an image, which only depends on one parameter and has the property of *causality*: That means it has to be insured, that features in coarse scale have always a reason in fine scale (Koenderink 1984). One can show, that a multi-scale representation based on a Gaussian function as low pass filter fulfils this requirement (Lindeberg 1994). In practice, the original signal $f(\vec{x})$ is convolved with a Gaussian kernel with an increasing scale parameter σ , the result of the convolution operation is assigned as $f(\vec{x}, \sigma)$. Small values of σ correspond to a fine scale level, large values to a coarse scale. An extensive investigation and mathematical reasoning including technical instructions can be found in (Lindeberg 1994).

One of the crucial problems from the position of object extraction is the estimation of the scale parameter σ , i.e. the selection of the scale level for the extraction of the low-level features. In (Schardt et al. 2002) it was proposed to use a scale selection mechanism, based on the maximum response after Scale-Space transformation; refer (Lindeberg 1998) for details. In our approach the scale selection is applied on a higher level, i.e. after the segmentation of the image, and not before, as it was proposed in (Schardt et al. 2002). This allows an internal evaluation of the segments on a semantic level, which is important if it is necessary to distinguish between trees and other objects.

3. DESCRIPTION OF THE APPROACH

The idea of the approach is to create a multi-scale representation of the surface model similar to (Persson et al. 2002). Here, the selection of the scale level is of crucial importance for the extraction of trees. On the one hand the correct scale level depends partly on the size of the objects one is looking for. But in the case of trees this size is neither known

a priori nor it is constant for all trees in one scene. On the other hand the correct scale is of crucial importance for the segmentation. In order to overcome this chicken-and-egg problem, the segmentation is performed in a wide range of scales, just bounded by reasonable values for the minimum and maximum diameter of a tree's crown.

The basis techniques of the approach are: the Linear Scale-Space Theory; the watershed transformation is used as segmentation technique, and Fuzzy Sets for the evaluation of the segments. The basic ideas of the Linear Scale-Space Theory were originally proposed in (Koenderink 1984), and were worked out in (Lindeberg 1994). Details about the watershed transformation can be found in (Soille 1999). Fuzzy Sets (Zadeh 1965) are used, because they are a “*very natural and intuitively plausible way to formulate and solve various problems in pattern recognition.*” (Bezdek 1992).

The necessity of a multi-scale approach for the extraction of trees from a surface model in Scale-Space $H(\vec{x}, \sigma)$ can be shown with the help of the magnitude of the surface model's gradient $|\nabla H(\vec{x}, \sigma)|$ and its Laplacian $\Delta H(\vec{x}, \sigma)$. The surface model $\Delta H(\vec{x}, 0)$ of a group of three trees is depicted in the left part of Figure 2 together with a height profile (dark grey line), the magnitude of the gradient (black line), and the Laplacian (light grey line) in the right part of the figure. The height profile and the corresponding derivatives were measured along the dotted line in the surface model. The same situation is depicted in Figure 3, but based on a slightly filtered surface model $\Delta H(\vec{x}, 3 m)$.

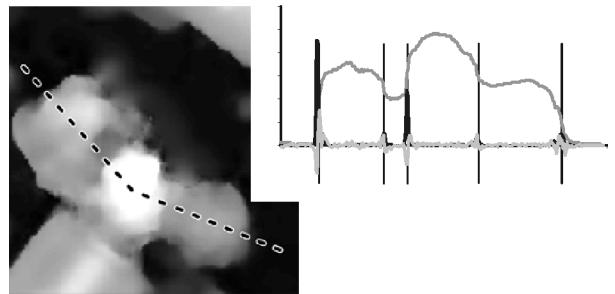


Figure 2: The surface model of three trees is depicted in the left part; in the right part the height profile along the dotted line, the magnitude of the gradient, and the Laplacian are depicted.

In the case of an analytical function like the geometrical part of the Pollock-Model the Laplacian is negative if the surface is konvex. In the case of the real surface of the trees the height profile of $\Delta H(\vec{x}, 0)$ is a little bit noisy, and as a result of this noise the Laplacian is oscillating close to zero, see Figure 2. In the “correct” scale level for this small group of trees the assumptions regarding the Laplacian are fulfilled quite well: The Laplacian is negative for trees (konvex surface) and positive for the valleys between them (Figure 3). Additionally, the coarse structure of the crown is enhanced. As a result of the transformation in Scale Space the properties of the Pollock-Model are valid for the real trees in this *correct* scale level.

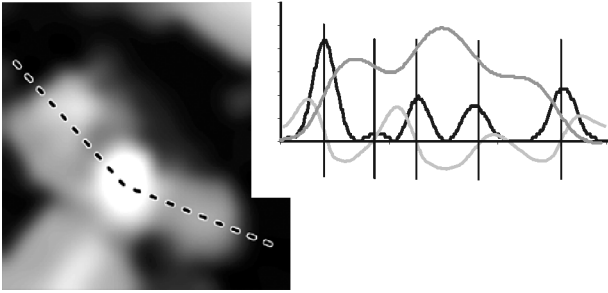


Figure 3: The surface model in the left part shows three trees filtered with a Gaussian (see Figure 2).

The correct scale level depends on the actual situation in the scene under investigation and cannot be predicted without detailed pre-knowledge about the scene. Therefore the segmentation is performed in a series of different scale levels, $\sigma = 2^n$, $n = 0, 0.5, 1.5, \dots, n_{\max}$, whereas n_{\max} is usually smaller than 5. Theoretically the upper bound does not influence the result, but only the computation time of the approach. The reason is that the size of the segments, which is influenced by the size of σ , is upper-bounded by the possible size of trees. And in turn the size is evaluated together with three other features in order to differentiate between trees and other objects in the investigated scene.

The strategy for the extraction of trees can be subdivided in two main phases, as depicted in Figure 4. First in the segmentation phase, a watershed transformation is performed in different scale levels of the surface model $H(\bar{x}, \sigma)$. In a second step the resulting segments $S_{\sigma, \bar{a}}$ were evaluated with the aim to classify them, i.e. to select those segments, which are *Tree_a*s. The image $I(\bar{x}, \sigma)$ enables the use of additional optical information in order to differentiate between trees and other high objects (buildings) in the scene.

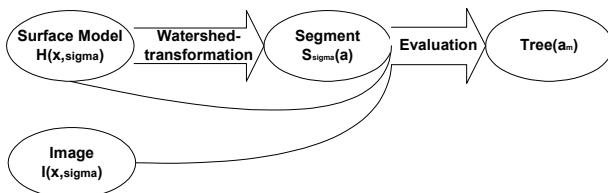


Figure 4: Strategy

The segmentation of the surface model is that part of the approach which depends heavy on the scale. As a consequence the segmentation procedure itself should be (1) free of parameters and (2) operate only in the image space and not in a feature space. The reason is, that a feature space has to be independent from the scale level for a low level operator. The watershed transformation fulfils these requirements. Additional, it is well suited for the segmentation of height data, because the key idea of the watershed transformation is a segmentation of an image by means of a flooding simulation (Soille 1999). *Basins* are the domains of the image, which are filled up first if a water level increases from the lowest grey value in the image; *Watersheds* are embankments between the Basins. This segmentation technique is also used in (Schardt et al. 2002) and a quite similar technique in (Persson et al. 2002) with the aim of detecting individual trees.

In the phase of segmentation every scale level $H(\bar{x}, \sigma)$ of the surface model $H(\bar{x})$ is subdivided into segments $S_{\sigma, \bar{a}}$. These segments are the *Basins* of the watershed transformation. If the watershed procedure is applied to extract trees, the surface model has to be transformed in such a way, that the trees itself are local minima. The easiest way to do this is to invert the surface model, as proposed in (Schardt et al. 2002). This works in forest areas, because there are usually narrow valleys between the individual crowns. In other areas like in settlement the situation may change, for example if trees occur in small groups; or if a way or a road occurs in forest areas. If these valleys are wide, the outlines of the basins are quite poor approximations of the crowns. Then it leads to better results to use the edges of the surface model as segmentation function. Good experiences have been made with the squared Laplacian $(\Delta H(\bar{x}, \sigma))^2$ as segmentation function in our experiments. Refer Figure 5 for an exemplary segmentation in three different scale levels.

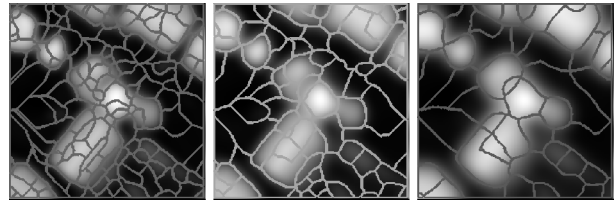


Figure 5: Basins of the watershed transform on three different scale levels

Finally, membership values were assigned to every segment $S_{\sigma, \bar{a}}$, which are partly derived from the segments itself (size and circularity), or the area belonging to the appropriate scale level $H(\bar{x}, \sigma)$ of the surface model (curvature), and the image $I(\bar{x}, \sigma)$ (\Leftrightarrow vegetation index or texture). This results in a feature vector \bar{a} consisting of four fuzzy membership values, which is assigned to every segment $S_{\sigma, \bar{a}}$. Four membership functions are used to transform the values of **circularity**, **convexity**, **size** and **vitality** into the corresponding membership values.

The membership function for the **circularity** $Area(B_\sigma) / r_{\max} \pi$ of a segment is depicted in Figure 6 (upper left). A sensible lower border is close to the value of 0.7 (circularity of square) and the upper border is 1 (circularity of a circle). The sign of the Laplacian of the surface model is used to discriminate between **convex** surfaces as trees and non-convex surfaces. For example, the surfaces of buildings and the most ground surfaces are plane, whereas the crown of a tree is a convex surface. Thus, a negative mean value of the Laplacian within the covered area of a segment leads to a membership value of 1, and in the case of a positive mean value the membership value is 0 (Figure 6, lower right).

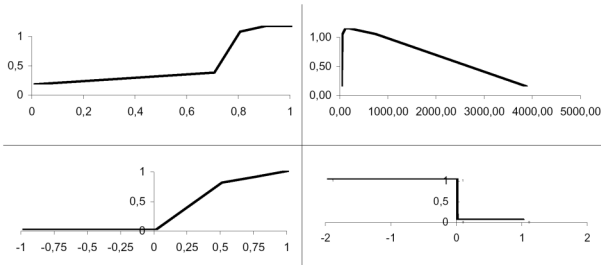


Figure 6: Membership functions

The following break points are used to define the membership function (Figure 6, upper right) for the **size** of a tree: The lower border is 20 m² according to a diameter of 2.5 m and the upper border is 700 m² (\Leftrightarrow 15 m). For larger values the membership value decreases, the largest possible diameter is assumed to be 35 m (\Leftrightarrow 3850 m²). These typical values for diameters cover all tree species, they can be found in (Gong et al. 2002). The feature **vitality** can be derived from an optional optical image $I(\bar{x}, \sigma)$, see Figure 4. It is used to discriminate between vegetation and non-vegetation areas. In the examples (see section 4 of this paper) the Normalized Difference Vegetation Index (NDVI) was used. High positive values are indicators for trees, negative values for buildings or roads – in any case not for vital vegetation. A membership function with an increasing membership values (Figure 6, lower left) for positive NDVI values is used with a break point at (0.5, 0.8).

It should be noted, that – except for the NDVI value, which depends in principle of the used sensor – all these parameters are object specific parameters, independent from the data.

The evaluation of the segments (refer Figure 4) consists of two steps. The first step is the evaluation of every segment $S_{\sigma, \bar{a}}$ based on its feature vector (refer Figure 7). This leads in some cases to valid hypothesis in different scale levels. These segments are covering each other in the image-plane. They are detected in the second step and the best one - according to its membership value - is selected as $Tree_{\bar{a}}$. A $Tree_{\bar{a}}$ is an object with a defined size, circularity, convexity AND vitality. Following the rules of the Fuzzy-Theorie, the minimum value of the feature vector is that value, which defines if a segment $S_{\sigma, \bar{a}}$ is classified as $Tree_{\bar{a}}$ or not.

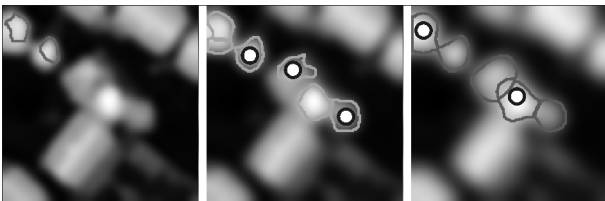


Figure 7: Valid hypotheses for trees in three different scales. The best hypotheses in scale space are marked with a white circle.

In some cases a valid hypothesis can occur at a more or less identical spatial position in the scene, but at different scale levels. In some cases these segments are quite similar in both depicted scale levels, and in some other cases the segments are subdivided in the finer scale level. The trivial case – a segment in just one scale – is rather an exception. These different situations of every segment have to be analysed. Hence, the type of the topological relation between the segments of

different scale levels has to be classified. If the topological relation is known, the best hypothesis for a tree can be selected at one and the same spatial position.

The classification of the topological relations between the valid segments is performed as proposed in (Winter 2000). In general, eight different topological relations exist in 2D space: *disjoint*, *touch*, *overlap*, *covers*, *contains*, *contained by*, *covers*, and *covered by* (Egenhofer & Herring 1991). These topological relations can be subdivided into two clusters $C1$ and $C2$, whereas the $C1$ cluster includes the relations *disjoint*, *touch* and $C2$ the other ones. The overlap relation is between these two clusters; it can be divided into *weak-overlap* ($C1$) and *strong-overlap* ($C2$) (Winter 2000). The motive behind this partitioning is that the relations in $C1$ are similar to *disjoint*, and in $C2$ to *equal*. We postulate that all the segments $S_A(\bar{a})$, which have a $C2$ topological relation to another segment $S_B(\bar{a})$ $A \neq B$, from another scale level, are potential hypothesis of the **same** tree in the real world. The best hypothesis - the one with the highest membership value - is selected as $Tree_{\sigma}(\bar{a})$ instance. These best hypotheses in scale space are marked with a white circle in Figure 7.

Finally, the gravity centre of a $Tree_{\sigma}(\bar{a})$ is used as position for the stem and the radius is computed based on the covered area of the selected segment.

4. PERFORMANCE EVALUATION

Recently, the approach was applied on those four different data sets, which were briefly described in the introduction of this paper. In this section we present first results of a performance evaluation of the approach. The test was carried out with one and the same set of membership functions for the features circularity, convexity, and size for all data sets. Only the vitality membership function was adapted to the different sensor data, the Hohentauern data set was processed without additional optical information.

In the last part of the previous section the procedure was described, which is used to detect a $C2$ relation between two objects on different scale levels. For the performance evaluation the same procedure is used to detect a 1:1 relation between a manually captured tree, assigned as $Tree_{REF}$ in the following, and an automatically extracted $Tree_{\sigma}(\bar{a})$. The acquisition of the reference data was performed on the basis of the same image data, which were used for the automatic procedure. It should be noted, that these reference data are a kind of an optimal result of what the approach should deliver from the developers point of view. The relationship between the manually captured reference and the trees in the real world is not discussed here. An investigation referring to this can be found in (Pollock 1996).

An extracted tree $Tree_{\sigma}(\bar{a})$ is assigned as True Positive (TP), if it has a topological relation from the $C2$ cluster with a tree from the manually captured reference, if not it is assigned as False Positive (FP). Those trees in the reference with a $C1$ relation to an extracted tree are assigned as False Negatives (FN). Based on these numbers, the *Completeness* C_{om} and the *Correctness* C_{orr} of the extraction result can be computed:

$$C_{om} = TP / (TP + FN) \quad C_{orr} = TP / (TP + FP) \quad (1)$$

In order to characterize the accuracy of the correct extracted trees, the arithmetic mean value and its standard deviation were computed for the distance between the centres of gravity and the radii between the $Tree_{REF}$, and the corresponding $Tree_{\sigma}(\bar{a})$.

The results for the four data sets are given in Table 1. The best results for the completeness were achieved for the Grangemouth and the Paris data set.

	C_{om} [%]	C_{orr} [%]	\overline{Pos} [m]	$\sigma_{\overline{Pos}}$ [m]	\overline{Rad} [m]	$\sigma_{\overline{Rad}}$ [m]
Grangemouth	96	81	1.1	0.8	-0.1	0.8
Hohentauern	70	86	1.1	0.8	-0.8	0.8
Paris	90	70	1.9	1.7	2.0	1.4
Ravensburg	50	59	1.4	1.0	-0.1	1.0

Table 1: Quality and accuracy

In the case of the Paris data set the accuracy of about 2 m for the position and the radius is quite poor, also the correctness of the extraction result is not really good. For a visual inspection of the results for the Paris data set refer Figure 8, examples of the Grangemouth data set are published in (Straub 2003a). A more detailed description of the results of the Hohentauern data set is given in (Straub 2003b). The values for the completeness of 70% and the correctness of 86% are inferior to the other examples, but it is in the same order of magnitude as it was reported for other approaches. For example in (Persson et al. 2002) the *Completeness* of 71% ($C_{orr}=100\%$) and in (Pollock 1996) 61% ($C_{orr}=85\%$) were achieved. Better results are reported in (Brandtberg & Walter 1998) ($C_{om}=85\%$, $C_{orr}=100\%$) and in (Andersen et al. 2001) namely $C_{om}=83\%$, and $C_{orr}=89\%$.



Figure 8: Subset of the Paris data set. Extracted trees are superimposed as white circles.

One reason for the poor results in the case of the Ravensburg data set is that it was acquired in April. Many trees were not

detected, due to the fact that the assumption of a high NDVI value was not fulfilled in this case. The correctness is bad, too. The poor performance of the approach in this case deserves closer attention; a corresponding investigation will be done in the near future.

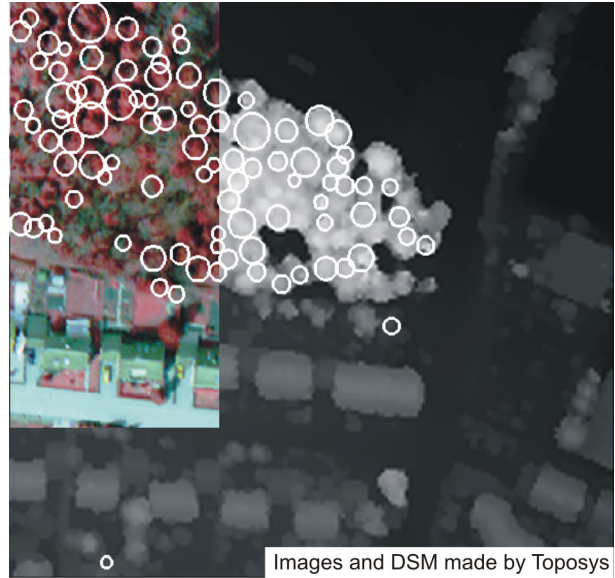


Figure 9: Subset of the Ravensburg data set. Extracted trees are superimposed as white circles.

5. SUMMARY AND OUTLOOK

In this paper an approach for the automatic extraction of trees is presented. The processing strategy is illustrated in detail. The approach is free of assumptions about the scale level, because the segmentation is performed in a wide range of different scale levels. The classification of the hypothesis is based on not more than four parameters: size, circularity, convexity, and vitality. From these four parameters only the vitality is depending on the used image material, the others are object properties. It should be noted, that the values for the size of the crowns stems from an independent investigation (Gong et al. 2002), and the convexity is always positive. Only the breakpoints in the circularity membership function are empirical values.

The approach was applied on four different data sets with the same set of parameters (except vitality) in order to demonstrate its general portability. The results are promising, even if there are problems in one of the data sets. This problem will be investigated in the near future.

Further developments should focus on the evaluation of the tree hypothesis. The highest potential is expected by a refinement of the membership functions with the help of statistical investigations on large data sets. The detection of the individual trees and the measurement of the outline can be looked upon as a bottleneck for the further classification of trees. Based on these, further information about the 3D shape of the crown or the fine structure characteristics of the individual tree can be extracted in the future.

ACKNOWLEDGEMENT

The European Commission under the contract IST-1999-10510 founded parts of this work.

The author would like to thank the French company ISTAR, which provided the Grangemouth and the Paris data sets. Many thanks also to the Joanneum Research in Graz for the Hohentauern data set, and the TopoSys GmbH, Germany, for making available the Ravensburg data set.

REFERENCES

- Andersen, H., Reutebusch, S. E., Schreuder, G. F., 2001. Automated Individual Tree Measurement through Morphological Analysis of a LIDAR-based Canopy Surface Model. *Proceedings of the First International Precision Forestry Cooperative Symposium*, University of Washington, Seattle, USA, , June 17-20, pp. 11-22.
- Andersen, H., Reutebusch, S. E., Schreuder, G. F., 2002. Bayesian Object Recognition for the Analysis of Complex Forest Scenes in Airborne Laser Scanner Data. *International Archives of the Photogrammetry, Remote Sensing and Spatial Information Sciences*, (eds.) Kallianly Leberl, ISPRS, Graz, Austria, Vol. XXXIV, Nr. WG 3A, pp. 35-41.
- Baltsavias, E., 1999. Airborne laser scanning: existing systems and firms and other resources. *ISPRS Journal of Photogrammetry and Remote Sensing*, 54 (1999), pp. 164-198.
- Bezdek, J. C., 1992. Computing with Uncertainty. *IEEE Communications Magazine*, September (1992), pp. 24-36.
- Brandtberg, T., Walter, F., 1998. Automated delineation of individual tree crowns in high spatial resolution aerial images by multiple scale analysis. *Machine Vision and Applications*, 11 (1998), pp. 64-73.
- Dralle, K., Rudemo, M., 1996. Stem Number Estimation by Kernel Smoothing of Aerial Photos. *Canadian Journal of Forest Research*, 26 (1996), pp. 1228-1236.
- Egenhofer, M. J., Herring, J. R., 1991. Categorizing Binary Topological Relations Between Regions, Lines, and Points in Geographic Databases. University of Maine, National Center for Geographic Information and Analysis, Orono, Maine, USA, pp. 28.
- Gong, P., Sheng, Y., Biging, G., 2002. 3D Model Based Tree Measurement from High-Resolution Aerial Imagery. *Photogrammetric Engineering & Remote Sensing*, 11 (68), pp. 1203-1212.
- Hill, D. A., Leckie, D. G., 1999. (eds.) *International forum: automated interpretation of high spatial resolution digital imagery for forestry, February 10-12, 1998*. Natural Resources Canada, Canadian Forest Service, Pacific Forestry Centre, Victoria, British Columbia, pp. 395.
- Koenderink, J., 1984. The Structure of Images. *Biological Cybernetics*, (50), pp. 363-370.
- Larsen, M., 1999. Individual tree top position estimation by template voting. 21. *Canadian Symposium on Remote Sensing*, Ottawa, Canada, 21-24 June, pp. 8.
- Lindeberg, T., 1994. *Scale-Space Theory in Computer Vision*. Kluwer Academic Publishers, Boston, USA, pp. 423.
- Lindeberg, T., 1998. Feature Detection with Automatic Scale Selection. *International Journal of Computer Vision*, 2 (30), pp. 79-116.
- Persson, A., Holmgren, J., Söderman, U., 2002. Detecting and Measuring Individual Trees Using an Airborne Laser Scanner. *Photogrammetric Engineering & Remote Sensing*, 9 (68), pp. 925-932.
- Pollock, R. J., 1994. A model-based approach to automatically locating tree crowns in high spatial resolution images. *Image and Signal Processing for Remote Sensing*, (eds.) Desachy, SPIE, Vol. 2315, pp. 526-537.
- Pollock, R. J., 1996. The Automatic recognition of Individual trees in Aerial Images of Forests Based on a Synthetic Tree Crown Image Model. *Dissertation Computer Science*, The University of British Columbia, Vancouver, Canada, June 1996, pp. 170.
- Schardt, M., Ziegler, M., Wimmer, A., Wack, R., Hyypä, R., 2002. Assessment of Forest Parameter by Means of Laser Scanning. *International Archives of the Photogrammetry, Remote Sensing and Spatial Information Sciences*, (eds.) Kallianly Leberl, ISPRS, Graz, Austria, Vol. XXXIV, Nr. 3A, pp. 302-309.
- Soille, P., 1999. *Morphological Image Analysis: Principles and Applications*. Springer, Berlin Heidelberg NewYork, pp. 316.
- Straub, B., 2003. Automatic Extraction of Trees from Aerial Images and Surface Models. *Proceedings of ISPRS Conference on Photogrammetric Image Analysis (PIA)*, (eds.) Baumgartner et al., ISPRS, München, Germany, September 17-19, pp. (accepted). (a)
- Straub, B., 2003. Automatic Extraction of Trees from Height Data using Scale Space and Snakes. *Second International Precision Forestry Symposium*, Precision Forestry Cooperative, Seattle, USA , 15.-18. Juni, pp. (in print). (b)
- Straub, B., Heipke, C., 2001. Automatic Extraction of Trees for 3D-City Models from Images and Height Data. *Automatic Extraction of Man-Made Objects from Aerial and Space Images*. Vol. 3. ed. Baltsavias Gruen van Gool, A.A.Balkema Publishers. Lisse Abingdon Exton(PA) Tokio. pp. 267-277.
- Winter, S., 2000. Uncertain Topological Relations between Imprecise Regions. *International Journal of Geographic Information Science*, 5 (14), pp. 411-430.
- Zadeh, L., 1965. Fuzzy Sets. *Information and Control*, 3 (8), pp. 338-353.